Hollow oxide formation by oxidation of Al and Cu nanoparticles

doi: 10.1063/1.2711383

Hollow oxide formation by oxidation of Al and Cu nanoparticles

R. Nakamura,[a] D. Tokozakura, and H. Nakajima
The Institute of Scientific and Industrial Research, Osaka University, Ibaraki, Osaka 567-0047, Japan

J.-G. Lee
Korea Institute of Machinery and Materials, Changwon-City 641-831, Korea

H. Mori
Research Center for Ultra-High Voltage Electron Microscopy, Osaka University, Ibaraki, Osaka 567-0047, Japan

(Received 2 October 2006; accepted 15 January 2007; published online 9 April 2007)

The formation of hollow metal oxide nanoparticles through the oxidation process at low temperatures from 295 to 423 K has been studied by transmission electron microscopy for Cu, Al, and Pb. For Cu and Al, hollow oxide nanoparticles are obtained as a result of vacancy aggregation in the oxidation processes, resulting from the rapid outward diffusion of metal ions through the oxide layer during the oxidation process. On the other hand, Pb nanoparticles turn to solid PbO because the diffusivity difference $D_{Pb} < D_O$ in PbO does not lend itself to the formation of vacancy clusters. The oxide growth behavior of Cu and Al nanoparticles of a larger size at 423 K are summarized as follows: (i) for Al, the rapidly forming oxide layer on its surface stops growing once it reaches a critical thickness of about 1.5 nm, (ii) the growth of Cu_2O continues until hollow Cu_2O of a certain thickness is formed. This suggests the occurrence of two different diffusion processes in the formation of hollow oxides: the rapid outward diffusion of metal ions based on the Cabrera–Mott theory plays an important role in the formation of hollow Al-oxides, whereas the Kirkendall effect at the Cu/Cu_2O interface, where Cu diffuses much faster than oxygen, brings about the formation of hollow Cu_2O. © *2007 American Institute of Physics*. [DOI: 10.1063/1.2711383]

I. INTRODUCTION

In recent years, considerable effort has been put into the design and fabrication of nanostructured materials with functional properties (e.g., nanoparticles, nanorods, etc.). Above all, it is important to obtain nanoparticles with a specific size and morphology, taking into consideration their specific applications. Therefore, the control of the shape of nanoparticles is one of the most important topics in the current research on nanomaterials.[1] In particular, there is an increasing interest in methods to fabricate hollow nanostructures because their unique shape makes them applicable to delivery vehicle systems, fillers, and catalysts, and could bring about changes in chemical, physical, and catalytic properties.[2–4] So far, various hollow spheres from different materials such as carbon,[5] polymers,[6] metals,[4,7] and inorganic materials[8] have been synthesized, mainly through chemical reaction processes.

More recently, it has been reported by Yin *et al.* that when isolated nanocrystals of cobalt are exposed to sulfur or oxygen at relatively low temperatures near 400 K, the initial solid nanocrystals turn to hollow spheres of cobalt sulfides or cobalt oxides.[9,10] They concluded that the formation mechanism of hollow spheres is based on the Kirkendall effect;[11] a nanohole in the center of the particles results from the generation and aggregation of vacancies due to different mobilities of ions moving in and out of the particles. Thereafter, the formation of hollow Fe-oxides[12] and ZnO[13] nanoparticles through the oxidation of Fe and Zn nanoparticles has been confirmed. It has been pointed out in both reports[12,13] that the rapid outward diffusion of the metal ions through a thin oxide layer at the initial oxidation stage plays an important role in the formation of hollow oxides via the oxidation reaction of Fe and Zn nanoparticles. However, there has been too few studies on the shape evolution of nanometer-sized metal particles and its governing factors to establish the mechanisms of hollow oxide formation associated with oxidation reactions. Thus, systematic studies on the oxidation-related morphology variation of nanoparticles are required, taking the kinetics of the oxidation processes of metal into consideration.

In the present work, the oxidation behavior of Cu, Al, and Pb nanoparticles and the formation of hollow structures are investigated comprehensively by transmission electron microscopy (TEM).

II. EXPERIMENT

Metal nanoparticles were prepared by evaporation in the specimen chamber of a transmission electron microscope.[14] A spiral-shaped tungsten filament was used as an evaporator and an amorphous carbon film was chosen as the supporting film (substrate), respectively. The distance between the evaporator and the supporting film was set to approximately 100 mm. The amorphous carbon film was mounted on a molybdenum grid and baked at 800 K for 600 s prior to evaporation in the TEM in order to avoid the contamination and oxidation of the metal nanoparticles during evaporation. Using the evaporator, Cu (99.99%), Al (99.999%), and Pb

[a]Author to whom correspondence should be addressed; electronic mail: rnakamur@sanken.osaka-u.ac.jp

(99.99%) were evaporated by Joule heating of the filament and deposited onto the supporting film under a base pressure below 5×10^{-5} Pa. The temperature of the supporting film during the evaporation was 773 K for Cu, 573 and 773 K for Al, and 473 K for Pb, respectively, in order to obtain the nanoparticles of a specific size between 5 and 50 nm. After evaporation, metal nanoparticles on the substrate were exposed to air and then heated at 295–423 K for a given time in air on the sample holder. Changes in the morphology and the structure of the metal nanoparticles associated with oxidation were observed by TEM.

The electron microscope used in the present work was a Hitachi H-800 TEM, operating at an accelerating voltage of 200 kV. It was equipped with a turbomolecular pump and a liquid N_2-cooled anticontamination device and a base pressure below 5×10^{-5} Pa was achieved.

III. RESULTS

A. Oxidation of Cu nanoparticles

A typical example of changes in the morphology and structure by oxidation of Cu nanoparticles is shown in Fig. 1. Figures 1(a) and 1(a′) show a bright field image (BFI) of as-deposited Cu nanoparticles on the substrate and the corresponding selected area electron diffraction (SAED) patterns, respectively. Debye–Scherrer (D–S) rings in the SAED are indexed as those of face-centered-cubic (fcc) copper. Figures 1(b) and 1(b′) show a BFI of Cu nanoparticles in the same area as Fig. 1(a) after oxidation at 373 K for 3.6 ks and the corresponding SAED patterns, respectively. By comparing Figs. 1(a) and 1(b), it is apparent that the size of the particles increases and the center part of the particle images becomes brighter after oxidation. It is suggested that initially solid Cu nanoparticles become hollow structures after oxidation. The D–S rings appearing in Fig. 1(b′) can be identified as Cu_2O (cuprite), indicating that hollow Cu_2O is formed via the oxidation of Cu nanoparticles. The mean diameter increases from 23.5 nm before oxidation to 32.0 nm after oxidation, indicating that the volume of the resulting hollow nanosphere is approximately 2.5 times larger than the initial metal nanoparticle as a result of oxidation. If solid Cu_2O were formed through the oxidation reaction, $2Cu+O\rightarrow Cu_2O$, the volume expansion from Cu to Cu_2O would be about 165%, taking into account the density and mass change. The extra volume expansion indicates that the outward mass transport occurs in the oxidation process and a void is produced in the particle.

Figure 2 shows BFIs of the morphology evolution of Cu nanoparticles with a diameter of about 30 nm oxidized at (a) 323 and (b) 373 K. In these images, the Cu_2O layers were distinctly observed surrounding the Cu nanoparticles. At the lower temperature of 323 K, the thickness of the Cu_2O layer increases from 3.0 nm for 0.6 ks to 6.5 nm for 72 ks, when the hollow structure is complete. On the other hand, at the higher temperature of 373 K, hollow Cu_2O is completely formed for 3.6 ks. The growth rate of the Cu_2O layer and the time required to reach hollow structures increase with the oxidation temperature, suggesting that a diffusion process with a large temperature dependence of mobility is operative

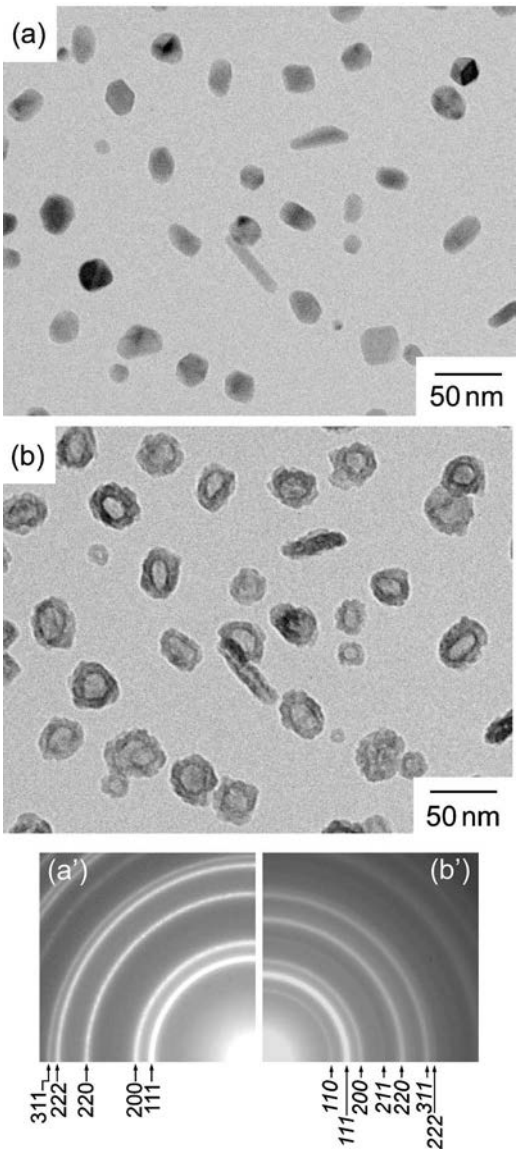

FIG. 1. Bright field images of Cu nanoparticles taken from the same area (a) as-deposited and (b) after oxidation at 373 K for 3.6 ks in air. (a′) and (b′) are their corresponding selected area electron diffraction patterns, respectively. Normal and italic numbers in (a′) and (b′) represent the plane indexes for Cu and Cu_2O_2, respectively.

in the oxidation of Cu nanoparticles. As shown in the BFI at 323 K for 24 ks and at 373 K for 1.2 ks, voids were observed at the interface between the inner Cu and outer Cu_2O layer in the course of oxidation, suggesting that the formation and condensation of vacancies occurred in the process of oxidation as was the case with Co.[9,10]

B. Oxidation of Al nanoparticles

Figure 3(a) shows a bright field image of Al nanoparticles which were deposited on a substrate kept at 573 K. The diameter of the particles ranged between 6 and 8 nm. The morphology change after exposure of the Al nanoparticles to air at 295 K for 120 s is shown in Fig. 3(b). The center part of almost all of the nanoparticles appears bright, indicating that Al nanoparticles became hollow spheres during the oxidation. In the SAED after oxidation of Al shown in Fig.

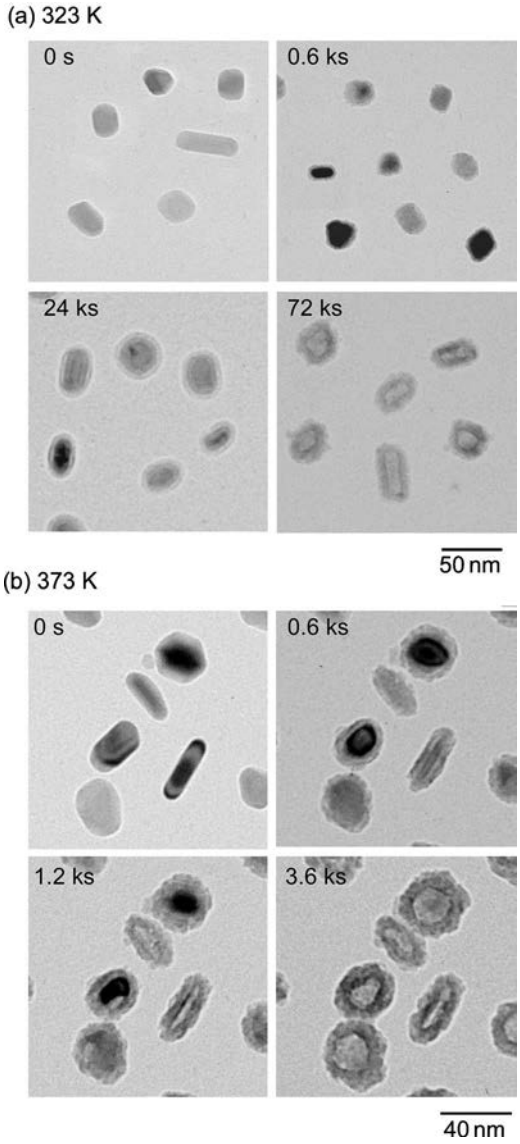

FIG. 2. BFIs of nanoparticle morphology before and during oxidation of Cu nanoparticles (a) at 323 K and (b) 373 K.

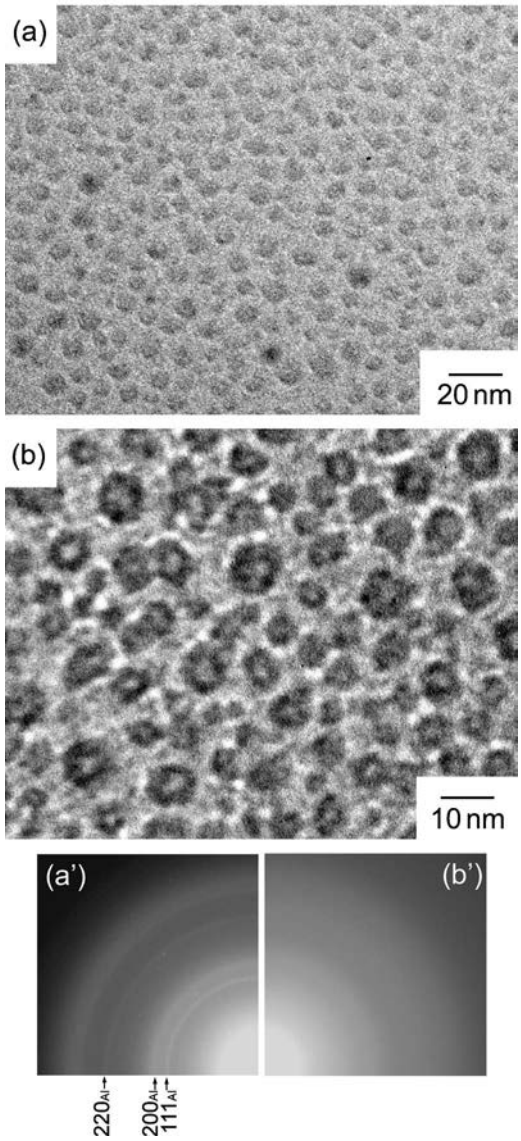

FIG. 3. BFIs of Al nanoparticles with 6 to 8 nm in diameter (a) as-deposited and (b) after exposure to air for a few minutes. Their corresponding SAED patterns are shown in (a′) and (b′), respectively.

3(b′), the Debye–Scherrer rings for fcc Al appearing in Fig. 3(a′) fully disappear and then halos appear after oxidation. These observations suggest that hollow amorphous oxide was formed by oxidizing smaller Al nanoparticles. The formation of amorphous oxide on the Al surface at low temperatures has been reported earlier.[15–17] Furthermore, the oxidation behavior of larger Al nanoparticles with 10−20 nm in diameter produced on a substrate kept at 773 K was investigated. Figure 4 shows a BFI of Al nanoparticles after oxidation at 423 K for (a) 3.6, (b) 36, and (c) 360 ks, respectively. The outline of the nanoparticles seems to be clear, indicating that a very thin oxidation layer is formed on the Al nanoparticles surface. However, the thickness of the oxide layer remains constant at about 1.5 nm regardless of increasing oxidation time. In the SAED patterns of the larger Al particles shown in Figs. 4(a′)–4(c′), Debye–Scherrer rings corresponding to fcc Al were observed, but those corresponding to crystalline Al-oxides were not observed. This suggests that the surface oxide layer formed on larger Al nanoparticles is not crystalline but amorphous and that the structure is kept even after a long period of oxidation. In the case of Al, it is difficult to observe the evolution of nanoparticles morphology associated with the oxidation reaction as observed for

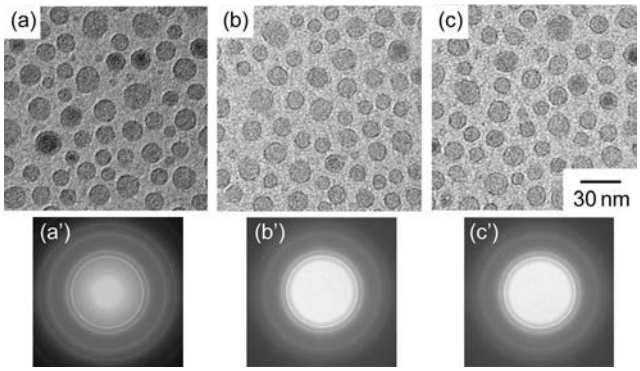

FIG. 4. BFIs and SAED patterns of Al nanoparticles with 10−20 nm in diameter after oxidation at 423 K for (a) 3.6, (b) 36, and (c) 360 ks. (a′)–(c′) are SAED patterns corresponding to (a)–(c), respectively.

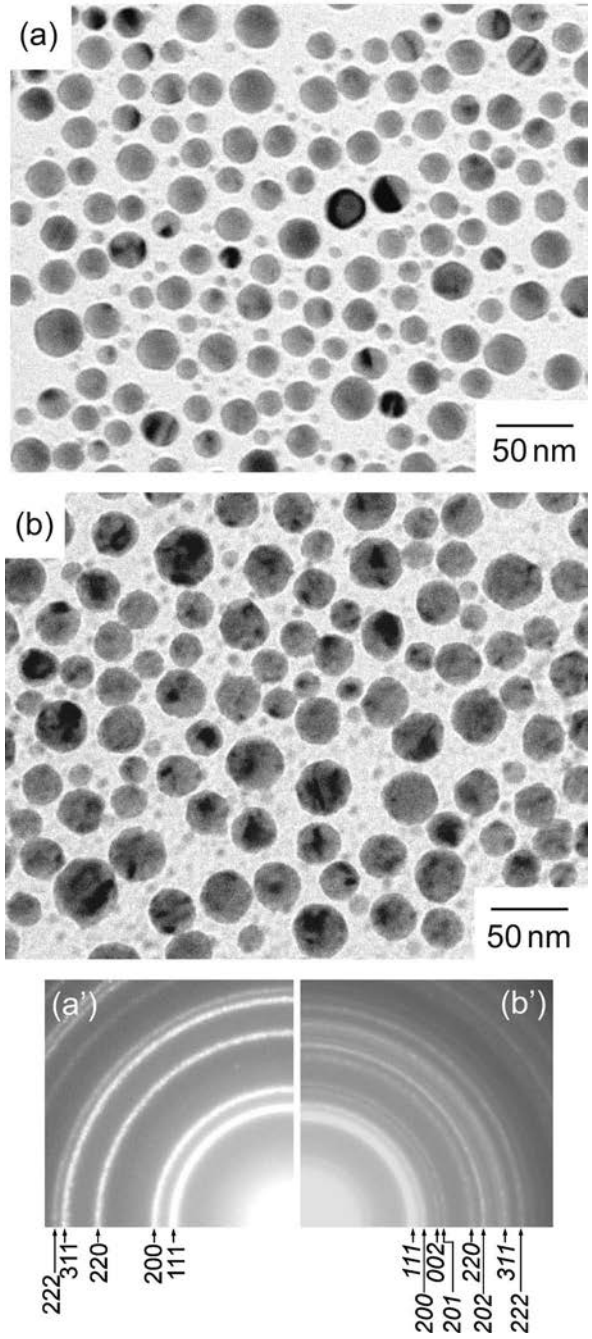

FIG. 5. A typical example for Pb nanoparticles before and after oxidation. (a) BFI of as-produced Pb nanoparticles. (b) BFI after oxidation at 423 k for 3.6 ks. Normal and italic numbers in (a′) and (b′) represent the plane indexes for Pb and PbO, respectively.

Cu (Fig. 2) since the formation of the initial oxidation layer is too rapid. As discussed later, this suggests that the diffusional process determining the hollow oxide formation in Al below 423 K is different from that of Cu.

C. Oxidation of Pb nanoparticles

Figure 5 shows BFIs of Pb nanoparticles (a) before and (b) after oxidation at 423 K for 3.6 ks and the corresponding SAED (a′) and (b′). From the BFI and SAED results, it is evident that Pb nanoparticles oxidized to tetragonal PbO and that no nanoholes were formed in the center of the particles.

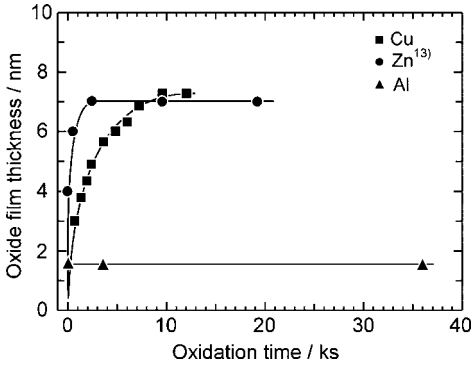

FIG. 6. Oxide-film thickness on the surface of Al and Cu nanoparticles as a function of oxidation time at 423 and 343 K, respectively. Data for Zn nanoparticles at 383 K are taken from our preceding study (see Ref. 12).

Through the oxidation reaction $Pb+O \rightarrow PbO$, the volume of the nanoparticles increased by about 40%. This is almost consistent with the 30% volume change estimated on the basis of the density and mass change.

D. Growth of oxide layer on Cu and Al

The thickness of the oxide layers formed on larger Cu and Al nanoparticles at 343 and 423 K, respectively, is plotted against the oxidation time in Fig. 6, together with the preceding results on Zn at 383 K.[13] The initial mean diameter of Cu, Al, and Zn before oxidation was 55, 20, and 50 nm, respectively. The thickness of the surface oxide layer on Al nanoparticles increases drastically with oxidation time at an early stage and then reaches a limiting thickness of 1.5 nm. The tendency of the oxide growth on the Al nanoparticles surface is in good agreement with that for bulk Al surfaces and the values of limiting thickness are almost consistent with each other.[17] As can be seen in Fig. 6, the oxidation behavior of Al is similar to that of Zn,[13] although the values of the limiting thickness differ. On the other hand, the thickness of Cu_2O on Cu increases rapidly with increasing oxidation time at an early stage. After that, it increases slowly with oxidation time and the thickness of Cu_2O finally reaches a limiting value. This result indicates that Cu atoms in the nanoparticles continue to react with oxygen as a result of outward diffusion of Cu ions through the Cu_2O layer until the hollow structure composed of a Cu_2O shell with a constant thickness is complete.

IV. DISCUSSION

Formation mechanisms of hollow oxides through the low-temperature oxidation of metal nanoparticles are discussed on the basis of the present results for Cu, Al, and Pb together with the preceding results of the oxidation of Zn.[13] It has been originally reported that the formation of hollow oxides through the oxidation of metal nanoparticles is due to the faster outward diffusion of metal ions compared to the inward diffusion of oxygen ions in the process of the formation of a surface oxide layer.[9,10] In the case of oxidation of Cu nanoparticles (see Figs. 1 and 2) and of Al nanoparticles smaller than 8 nm at 295 K (see Fig. 3) in air, hollow oxides particles are formed. Such a morphology change seems to

result from the faster outward migration of Cu and Al ions through their oxide layers than that of inward oxygen ions, as is the case with Co,[9,10] Fe,[12] and Zn.[13] The faster outward diffusion of metal ions from the core metal to the outer oxide shell produces excess vacancies at the metal side near the metal/oxide interface. Vacancy clusters begin to be formed at the interface in the course of oxidation and become larger as the metal atoms in the core migrate into the oxide layer and then contribute to the formation of a new oxide layer. After all metal ions are consumed by the reaction with the oxygen ions absorbed on the oxide surface, a nanopore is formed as a result of vacancy clustering in the core of the oxide particle.

In contrast, hollow PbO nanoparticles do not form through the oxidation of Pb nanoparticles, as shown in Fig. 4. It has been well understood that the anodic corrosion of Pb occurs as a result of oxygen penetration through the PbO and PbO_2 layers toward Pb;[18–20] the inward diffusion of the oxygen anions is faster than the outward diffusion of Pb cations at the interface between Pb and PbO. Under the conditions the ion transport take place, vacancies do not pile up near the interface between Pb and PbO because vacancies at the interface can be filled by the inward flow of O ions from the PbO side. Unlike the oxidation of Cu, Zn, and Al nanoparticles, the interface between Pb and PbO moves inward because of the faster migration of oxygen ions from the outer oxygen to the inner oxides scale, resulting in the formation of solid PbO nanoparticles. The result for Pb, which is different from that for Cu, Al, and Zn,[13] suggests that the faster outward diffusion of metal ions through the oxide layer is essential for the formation of hollow oxide particles via the oxidation reaction.

In this section, the dominant diffusional processes in the formation of hollow oxide nanoparticles will be discussed on the basis of a comparison between the oxidation behavior of Cu and Al. It is well known that a characteristic feature of low-temperature oxidation of a large number of metals is that the oxidation rate is initially very rapid and that it gradually drops off to very low levels.[21] According to Cabrera and Mott,[22] the low-temperature oxidation theory is based on the assumption that oxygen atoms are adsorbed on the oxide surface and that electrons can pass rapidly through the oxide by tunneling to establish an equilibrium between the metal and adsorbed oxygen. This process creates an electronic field in the thin oxide layer capable of pulling metal ions through the oxide film. As a result, it decreases the activation energy for the migration of metal ions, i.e., it facilitates the transport of metal ions across the oxide film. After the formation of an initial oxide layer of a certain thickness, thermally activated ion migration is necessary for the further growth of the oxide layer.[22,23] As can be seen in Fig. 6, the growth of the oxide layers of Al and Zn nanoparticles stops for practical time ranges after the rapid formation of initial oxide layers whereas the growth of Cu_2O layer on Cu surface continues until the hollow structure composed of a Cu_2O shell with a constant thickness is complete, indicating that the oxidation behavior of Al and Zn differs from that of Cu after the formation of an initial oxide layer at around 400 K.

Figure 7 shows the temperature dependence of self-diffusion coefficients for the metal and the oxygen ions in Cu_2O,[24,25] ZnO,[26,27] and α-Al_2O_3.[28,29] (The solid and broken lines correspond to the temperature range of experimental measurements by each worker and of its extrapolation, respectively.) The data on α-Al_2O_3 are shown for reference, since diffusion data in amorphous Al-oxide are unavailable. There is a common characteristic that self-diffusion coefficients of metal ions are much larger than those of oxygen ions in Cu_2O, ZnO, and α-Al_2O_3 mainly because the radius of the metal ions is significantly smaller than that of the oxygen ions in these oxides.[21] However, the absolute value of the diffusion coefficient of Cu_2O are much higher compared to those of ZnO and Al_2O_3. The difference of diffusivity in the oxides seems to originate mainly in the difference in the strength of ionic bonding and the formation behavior of point defects due to the deviation from stoichiometry.[21] As discussed in a preceding article,[13] the average diffusion distance is estimated to be of the order of 10^{-14} m at 423 K, which is considerably less than 10^{-9} m. The low mobility of Zn ions in ZnO by a thermal-activated vacancy mechanism at around 400 K can explain the experimental result that the growth of ZnO layer on the larger Zn nanoparticles ($\sim$50 nm) stops for practical time ranges after the formation of the initial oxidation layer. As expected from the extrapolated line in Fig. 7, the self-diffusion coefficient of Al in Al_2O_3 at around 400 K is far smaller than that of ZnO. Thus, the growth of the oxide layer on Al by a thermal-activated vacancy mechanism can be neglected for practical time ranges at low temperatures at around 423 K after the rapid formation of the initial oxide layer of about 1.5 nm in thickness at the initial oxidation stage, where the kinetics proposed by Cabrera–Mott seem to be dominant. It has been already recognized that the initial oxidation process is operative for the formation of hollow Fe (Ref. 12) and Zn (Ref. 13) oxides via the oxidation of smaller nanoparticles of about

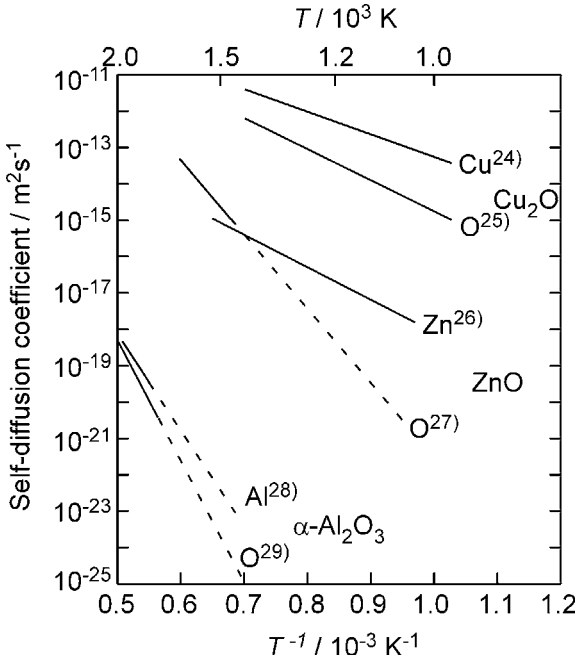

FIG. 7. Self-diffusion coefficients of both metal and oxygen ions in Cu_2O, ZnO, and α-Al_2O_3 as a function of the reciprocal temperature.

TABLE I. Critical diameter for obtaining hollow oxide nanospheres from oxidation of metal nanoparticles at low temperature as low as 423 K. In the case of Al and Zn (Ref. 12) the final morphology (hollow oxide or metal nanoparticle with oxide layer) depends on the critical thickness based on the CM theory. In the case of Cu, hollow oxide nanospheres can be obtained between 10 and 40 nm as D_{Cu} is much larger than D_O in Cu_2O. For Pb, solid oxide nanoparticles are obtained because of $D_{Pb} < D_O$ in PbO.

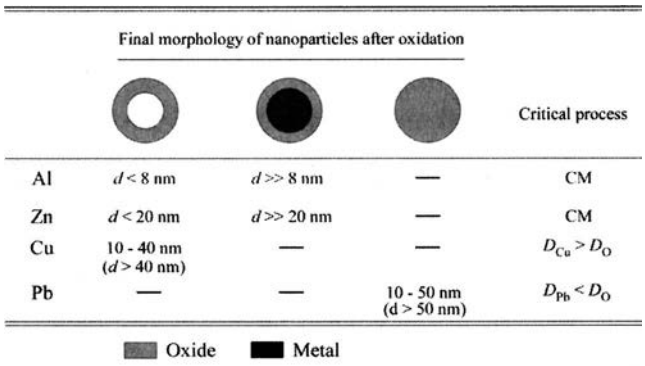

8 and 20 nm in diameter, respectively. It can be concluded that the rapid outward diffusion of metal cations at the initial oxidation stage based on the Cabrera–Mott theory plays an important role in the formation of hollow Al-oxide through oxidation of Al nanoparticles smaller than 8 nm at low temperatures below 423 K.

On the other hand, the self-diffusion coefficients of Cu ions, D_{Cu}, in Cu_2O at 373 and 323 K are calculated to be 1.8×10^{-24} and 4.7×10^{-27} m^2 s^{-1}, respectively, using the Arrhenius parameters obtained by Peterson and Wiley.[24] The average diffusion distance, $\sqrt{D_{Cu}t}$, at 373 K for 3.6 ks and at 323 K for 72 ks is estimated to be 8×10^{-11} and 2×10^{-11} m, which are one to two orders of magnitude smaller than 10^{-9} m. However, the effect of the electric field on the promotion of Cu migration through the oxide layer cannot be neglected after the formation of an initial oxide layer although the effect becomes weaker as the oxide layer grows. Therefore, it seems likely that Cu ions have sufficient mobility to make the oxide layer grow by a thermal activated vacancy mechanism unlike the oxidation of Al and Zn; the Kirkendall effect at the Cu/Cu_2O interface, where Cu diffuses much faster than oxygen, is a dominant process for the formation of hollow Cu_2O. Hollow Cu_2O are expected to be produced at temperatures as low as 373 K in practical time ranges regardless of the initial particle diameter of Cu.

Finally, the critical diameters for obtaining hollow oxide nanoparticles from the oxidation of metal nanoparticles at temperature as low as 423 K are summarized in Table I in terms of the dominant oxidation process determining the final morphology of the nanoparticles. In the case of Al and Zn (Ref. 13) the final morphology (hollow oxide or metal nanoparticle with oxide layer) depends on the critical thickness based on the Cabrera–Mott (CM) theory. In the case of Cu, hollow oxide nanoparticles can be obtained between 10 and 40 nm as D_{Cu} is considerably larger than D_O in Cu_2O. For Pb, solid oxide particles are obtained because of $D_{Pb} < D_O$ in PbO.

V. CONCLUSIONS

The oxidation behavior of Cu, Al, and Pb nanoparticles and the formation of hollow structures were investigated by TEM. The following conclusions were obtained from this study.

(a) Cu nanoparticles of diameters ranging from 10 to 40 nm were observed to become hollow Cu_2O particles after oxidation at 373 K for 3.6 ks. The exposure of Al nanoparticles with diameters smaller than 8 nm to air led to the formation of hollow amorphous particles, although the thin film amorphous oxide of 1.5 nm in thickness which formed on larger Al nanoparticles was stable against long-time oxidation at 423 K.

(b) Solid PbO nanoparticles were produced by oxidizing Pb nanoparticles because inward oxygen diffusion through the oxide layer is the rate-determining process. This result clearly demonstrates that faster outward diffusion of metal ions through the oxide layer yields the formation of hollow oxide particles via oxidation processes.

(c) In the case of the oxidation of smaller Al nanoparticles, the rapid outward migration of metal ions at the initial oxidation stage makes hollow amorphous oxide particles. However, larger hollow Al-oxide nanoparticles could not be formed by thermal oxidation because the growth of the oxide layer stops after the formation of the initial oxidation layer. On the other hand, the self-diffusion coefficient of Cu ions in Cu_2O at 373 K is high enough to explain the growth of the Cu_2O layer via the thermal-activated diffusion process after the initial oxide formation.

ACKNOWLEDGMENTS

The authors express their appreciation to Dr. W. Sprengel of Glatz University, Austria, for helpful discussion. This work was supported by Grant-in-Aid for Scientific Research (Category S) and the 21st Century COE Program (Toward Creating New Industries Based on Inter-Nanoscience) from the Ministry of Education, Culture, Sports, Science and Technology of Japan, and also by the Iketani Science and Technology Foundation.

[1] Y. Xia and N. J. Halas, MRS Bull. **30**, 356 (2005).
[2] S. W. Kim, M. Kim, W. Y. Lee, and T. Hyeon, J. Am. Chem. Soc. **124**, 7642 (2002).
[3] Y. Sun and Y. Xia, J. Am. Chem. Soc. **126**, 3892 (2004).
[4] Y. Deng, L. Zhao, B. Shen, L. Liu, and W. Hu, J. Appl. Phys. **100**, 014304 (2006).
[5] J. Lee, K. Sohn, and T. Hyeon, J. Am. Chem. Soc. **123**, 5146 (2001).
[6] T. K. Mandal, M. S. Fleming, and D. R. Walt, Chem. Mater. **12**, 3481 (2000).
[7] C. Graf and A. Blaaderen, Langmuir **18**, 524 (2002).
[8] F. Caruso, R. A. Caruso, and H. Möhwald, Science **282**, 1111 (1998).
[9] Y. Yin, R. M. Robert, C. K. Erdonmez, S. Hughes, G. A. Somorjai, and A. P. Alivisatos, Science **304**, 711 (2004).
[10] Y. Yin, R. M. Robert, C. K. Erdonmez, S. Hughes, G. A. Somorjai, and A. P. Alivisatos, Adv. Funct. Mater. **16**, 1389 (2006).
[11] A. D. Smigelskas and E. O. Kirkendall, Trans. AIME **171**, 130 (1947).
[12] C. M. Wang, D. R. Baer, L. E. Thomas, J. E. Amonette, J. Antony, Y. Qiang, and G. Duscher, J. Appl. Phys. **98**, 094308 (2005).
[13] R. Nakamura, J.-G. Lee, D. Tokozakura, H. Mori, and H. Nakajima, Mater. Lett. **61**, 1060 (2007).
[14] J.-G. Lee, H. Mori, and H. Yasuda, J. Mater. Res. **20**, 1708 (2005).
[15] M. J. Dignam, W. R. Fawcett, and H. Bohni, J. Electrochem. Soc. **113**, 656 (1966).

[16]M. Martin and E. Fromm, Thin Solid Films **236**, 199 (1993).
[17]L. P. H. Jeurgens, W. G. Sloof, F. D. Tichelaar, and E. J. Mittemeijer, J. Appl. Phys. **92**, 1649 (2002).
[18]B. A. Thompson and R. L. Strong, J. Phys. Chem. **67**, 594 (1963).
[19]D. Pavlov, Electrochim. Acta **23**, 845 (1978).
[20]T. Laitinen and J. P. Pohl, Electrochim. Acta **34**, 377 (1989).
[21]P. Kofstad, *High-Temperature Oxidation of Metals* (Wiley, New York, 1966), p. 41.
[22]N. Cabrera and N. F. Mott, Rep. Prog. Phys. **12**, 163 (1948–1949).
[23]K. R. Lawless, Rep. Prog. Phys. **37**, 231 (1974).
[24]N. L. Peterson and C. L. Wiley, J. Phys. Chem. Solids **45**, 281 (1984).
[25]W. J. Moore, Y. Ebisuzaki, and J. A. Sluss, J. Phys. Chem. **62**, 1438 (1958).
[26]W. J. Moore and E. L. Williams, Discuss. Faraday Soc. **28**, 86 (1959).
[27]J. W. Hoffman and I. Lauder, Trans. Faraday Soc. **66**, 2346 (1970).
[28]M. L. Gall and B. Lesage, Philos. Mag. A **70**, 761 (1994).
[29]D. Prot and C. Monty, Philos. Mag. A **73**, 899 (1996).